Image gathers of SV-waves in homogeneous and factorized VTI media

Ramzy M. Al-Zayer[1] and Ilya Tsvankin[2]

ABSTRACT

Reflection moveout of SV-waves in transversely isotropic media with a vertical symmetry axis (VTI media) can provide valuable information about the model parameters and help to overcome the ambiguities in the inversion of P-wave data. Here, to develop a foundation for shear-wave migration velocity analysis, we study SV-wave image gathers obtained after prestack depth migration.

The key issue, addressed using both approximate analytic results and Kirchhoff migration of synthetic data, is whether long-spread SV data can constrain the shear-wave vertical velocity V_{S0} and the depth scale of VTI models. For homogeneous media, the residual moveout of horizontal SV events on image gathers is close to hyperbolic and depends just on the NMO velocity V_{nmo} out to offset-to-depth ratios of about 1.7. Because V_{nmo} differs from V_{S0}, flattening moderate-spread gathers of SV-waves does not ensure the correct depth of the migrated events.

The residual moveout rapidly becomes nonhyperbolic as the offset-to-depth ratio approaches two, with the migrated depths at long offsets strongly influenced by the SV-wave anisotropy parameter σ. Although the combination of V_{nmo} and σ is sufficient to constrain the vertical velocity V_{S0} and reflector depth, the tradeoff between σ and the Thomsen parameter ϵ on long-spread gathers causes errors in time-to-depth conversion. The residual moveout of dipping SV events is also controlled by the parameters V_{nmo}, σ, and ϵ, but in the presence of dip, the contributions of both σ and ϵ are significant even at small offsets.

For factorized $v(z)$ VTI media with a constant SV-wave vertical-velocity gradient k_{zs}, flattening of horizontal events for a range of depths requires the correct NMO velocity at the surface, the gradient k_{zs}, and, for long offsets, the parameters σ and ϵ. On the whole, the nonnegligible uncertainty in the estimation of reflector depth from SV-wave moveout highlights the need to combine P- and SV-wave data in migration velocity analysis for VTI media.

INTRODUCTION

Velocity model-building for seismic imaging is usually implemented as an iterative process that includes migration followed by velocity analysis and model updating. Most existing migration velocity analysis algorithms are designed for P-waves in heterogeneous isotropic media (e.g., Al-Yahya, 1987; Liu, 1997). The improved quality of multicomponent data acquired offshore in ocean-bottom cable (OBC) surveys, however, has prompted the development of processing methods operating with shear-wave (mostly mode-converted) data (e.g., Thomsen, 1999; Grechka and Tsvankin, 2002a; Grechka et al., 2002; Grechka and Dewangan, 2003). Since seismic anisotropy typically has a much stronger influence on S-waves than on P-waves, isotropic velocity models are seldom adequate for shear-wave imaging, as evidenced by widespread mis-ties between PP and PS (or SS) migrated sections (Thomsen, 1999; Tsvankin, 2001).

The high sensitivity of shear waves to the presence of anisotropy is an important asset in constraining the anisotropic parameters using reflection data. For transversely isotropic media with a vertical axis of symmetry (VTI media), P-wave reflection traveltimes alone usually are insufficient for estimating reflector depth and Thomsen's anisotropic parameters ϵ and δ. As shown by Alkhalifah and Tsvankin (1995), all P-wave time-domain signatures for models with a laterally homogeneous VTI overburden are controlled by the NMO velocity of horizontal events and the anellipticity parameter $\eta \equiv (\epsilon - \delta)/(1 + 2\delta)$. Supplementing P-wave data with conventional-spread (hyperbolic) moveout of SV-waves or with long-spread converted PSV data still does not result in a stable procedure for estimating ϵ, δ, and the vertical P- and S-wave velocities V_{P0} and V_{S0} (Grechka and Tsvankin, 2002b).

To overcome the ambiguity in the inversion of reflection data, Tsvankin and Thomsen (1995) suggest combining

long-spread P- and SV-wave traveltimes from horizontal interfaces. They demonstrate that the strongly nonhyperbolic SV-wave moveout in directions close to the velocity extremum (i.e., near 45° incidence angle) helps to constrain the velocity V_{S0} and reconstruct the vertical scale of the model. For multilayered media, the joint time-domain inversion of P- and SV-wave data may be performed in a layer-stripping mode.

For subsurface models with vertical and lateral heterogeneity, however, it is preferable to carry out parameter estimation by means of migration velocity analysis (MVA), which operates with reflection data after prestack depth migration. An MVA algorithm for P-wave data in VTI media is presented by Sarkar and Tsvankin (2003, 2004), who identify the parameter combinations needed to flatten P-wave events in migrated (image) gathers and place them at the correct depth. In addition to homogeneous models, they study factorized $v(x, z)$ VTI media in which V_{P0} varies linearly in both vertical and horizontal directions but the anisotropic parameters and the V_{P0}/V_{S0} ratio are constant. One of their conclusions is that although the vertical gradient in V_{P0} is constrained by P-wave traveltimes, a unique reconstruction of the anisotropic velocity field from P-wave data still requires a priori information about the vertical velocity or reflector depth.

The goal of this work is to analyze the information contained in the moveout of long-spread SV events in image gathers. Since correlating P and SV reflection events on field data is not an easy task, it is important to learn if SV-waves alone can be used to determine reflector depth in VTI media. By employing analytic expressions and performing actual depth migration, we identify the combinations of model parameters needed to accurately image shear-wave data. The results can be used in MVA algorithms operating with multicomponent (P and SV) data from heterogeneous VTI media.

REFLECTION MOVEOUT OF P- AND SV-WAVES IN VTI MEDIA

Here, we briefly review some key differences between the kinematics of P and SV reflections in VTI media. Figure 1 shows phase velocity as a function of phase angle in Taylor sandstone; the model parameters are taken from Thomsen (1986). As is the case for typical VTI media, the P-wave phase velocity increases almost monotonically with angle from V_{P0} to the horizontal velocity V_{hor} with only a shallow minimum

in between. The SV-wave curve, in contrast, reaches a distinctive maximum at an angle slightly smaller than 45°. The magnitude of this maximum, and of SV-wave velocity anisotropy in general, is largely governed by the parameter σ, defined by Tsvankin and Thomsen (1994) as

$$\sigma \equiv \frac{V_{P0}^2}{V_{S0}^2}(\epsilon - \delta). \qquad (1)$$

If $\sigma < 0$ (not a typical case), the SV-wave velocity has a minimum near 45° and maxima in the vertical and horizontal directions.

Since the ratio V_{P0}/V_{S0} could be as high as three, σ can be almost ten times larger in magnitude than ϵ or δ. The parameter σ is responsible not only for the phase-velocity variation of SV-waves but also for the difference between the SV-wave NMO velocity in a horizontal VTI layer (V_{nmo}) and the vertical velocity:

$$V_{nmo} = V_{S0}\sqrt{1 + 2\sigma}. \qquad (2)$$

The different character of the phase-velocity functions in Figure 1 leads to substantial differences in the moveout ($t^2 - x^2$) curves for the two waves (Figure 2). Although the traveltimes in Figure 2 are computed at equal phase-angle increments, the density of rays (and of receiver locations) is higher near the velocity maxima of both modes. With increasing offset, the influence of anisotropy causes the exact traveltimes to diverge from the hyperbolic moveout curves parameterized by the analytic NMO velocity. Note that the deviation of the P-wave curve increases gradually with offset, whereas the SV-wave curve stays hyperbolic out to larger offset-to-depth ratios ($x/z \approx 1.7$) and then sharply diverges from the hyperbola.

As discussed in Tsvankin and Thomsen (1994) and Tsvankin (2001), P-wave moveout becomes nonhyperbolic at smaller offsets because the magnitude of the quartic moveout coefficient is usually larger for P-waves than for SV-waves (if $\sigma > 0$). The abrupt departure of the SV-wave moveout from the hyperbola at $x/z > 1.7$ is caused by the influence of the velocity maximum. Such a behavior of SV-wave moveout, which is not well described by the quartic Taylor series or the Tsvankin-Thomsen (1994) nonhyperbolic equation, has serious implications for MVA on long-spread image gathers (see
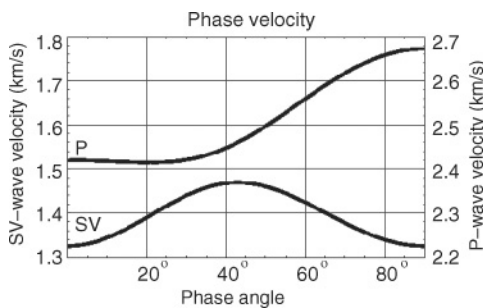

Figure 1. Phase velocity of P- and SV-waves in Taylor sandstone as a function of the phase angle from the vertical. The model parameters are $V_{P0} = 2.420$ km/s, $V_{S0} = 1.325$ km/s, $\epsilon = 0.11$, and $\delta = -0.035$.
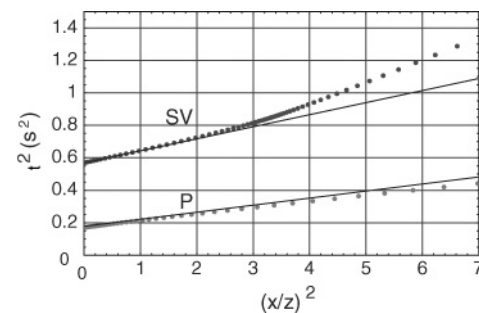

Figure 2. Squared traveltime (dots) as a function of the squared offset-to-depth ratio for P- and SV-waves in Taylor sandstone (computed at equal phase-angle increments). The solid lines mark the hyperbolic moveout curves parameterized by the NMO velocity.

following). While deviation from hyperbolic moveout for both P- and SV-waves is related to the anellipticity of the model (i.e., to the difference $\epsilon - \delta$), the parameter combinations that control the magnitude of nonhyperbolic moveout are different: η for P-waves and σ for SV-waves.

ANALYSIS OF SV-WAVE IMAGE GATHERS

Modeling and migration algorithms

The image gathers used for the following numerical analysis were computed by migrating 2D synthetic data from homogeneous and vertically heterogeneous [factorized $v(z)$] VTI media. To generate synthetic seismograms, we adapted for SV-waves a dynamic ray-tracing program written by Alkhalifah (1995a) for P-waves in factorized VTI media; the original code, susynlvfti, is available in Seismic Unix (SU), a software package developed by the Center for Wave Phenomena at Colorado School of Mines.

Prestack migration was performed using the Kirchhoff SU code sukdmig2d developed by Liu (1997) for isotropic media; the only change required to migrate SV data in VTI media was in using the appropriate traveltime table. The traveltimes for SV-waves were computed by adapting Alkhalifah's (1995b) anisotropic P-wave ray-tracing code, rayt2dan. Note that the work of Sarkar and Tsvankin (2003, 2004) for P-wave data is based on the same three SU codes cited here.

Homogeneous VTI medium

SV-wave propagation in VTI media is controlled by four Thomsen parameters: V_{P0}, V_{S0}, ϵ, and δ. For purposes of SV-wave moveout analysis, however, it is convenient to replace the two vertical velocities by the SV-wave NMO velocity V_{nmo} for horizontal interfaces (equation 2) and the parameter σ (equation 1). Therefore, the parameter set used in our tests includes V_{nmo}, σ, ϵ, and δ.

Horizontal events

Consider a horizontal reflector embedded in a homogeneous VTI medium (Figure 3). For P-waves, the weak-anisotropy approximation for the residual moveout of horizontal reflection events in image gathers is derived by Sarkar and Tsvankin (2003, their Appendix A). As discussed in Tsvankin (2001), all kinematic signatures of SV-waves in the weak-anisotropy limit can be adapted from the corresponding P-wave signatures by replacing V_{P0} with V_{S0}, and δ with σ, and by setting ϵ to zero. Therefore, we obtained the residual-

moveout formula for SV-waves by applying these substitutions to equation A-10 of Sarkar and Tsvankin (2003):

$$z_M^2(h) \approx r^2 z_T^2 + h^2 V_{S0,M}^2 \left(\frac{1}{V_{nmo,T}^2} - \frac{1}{V_{nmo,M}^2} \right)$$
$$- \frac{2h^4}{h^2 + z_T^2} \left(\sigma_M \frac{V_{nmo,T}^2}{V_{nmo,M}^2} - \sigma_T \frac{V_{nmo,M}^2}{V_{nmo,T}^2} \right), \quad (3)$$

where the subscript T refers to the true model and M to the migration model, z_M is the migrated depth, z_T is the true depth, h is half the source-receiver offset, and $r \equiv V_{S0,M}/V_{S0,T}$ is the ratio of migration and true vertical velocities. The first term $(r^2 z_T^2)$ in the approximate equation 3 depends just on the vertical velocity and gives the correct zero-offset migrated depth if $V_{S0,M} = V_{S0,T}$. The rest of the equation describes offset-dependent residual moveout, with the quadratic term controlled by the NMO velocity and the quartic (nonhyperbolic) term influenced by both V_{nmo} and σ.

According to equation 3, using the correct V_{nmo} and σ in the migration process not only removes residual moveout but also positions the reflector at the true depth. Indeed, it is clear from equation 2 that a model with the correct values V_{nmo} and σ must have the correct vertical velocity V_{S0} as well. In contrast, flattening P-wave image gathers in VTI media does not guarantee the correct depth scale of the section (Sarkar and Tsvankin, 2003) because P-wave residual moveout depends on the NMO velocity and the parameter η — a parameter combination that does not constrain the vertical velocity V_{P0}.

The absence of the parameters ϵ and δ in equation 3 is a consequence of using the weak-anisotropy approximation. To study the dependence of SV-wave image gathers on ϵ and δ, we derived an exact residual-moveout equation for horizontal SV events in homogeneous VTI media with the help of symbolic software Mathematica. Although this expression is too lengthy to be given here, it allows us to model residual moveout without performing depth migration and to evaluate the sensitivity of SV-wave moveout to the model parameters (Figure 4).

From Figure 4, both ϵ and δ have some influence on the residual moveout at large offsets. For small and moderate offset-to-depth ratios up to $x/z \approx 1.7$, the SV moveout is fully
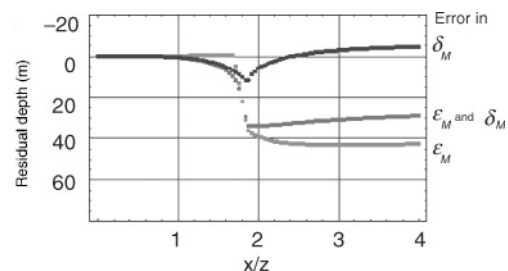
Figure 3. True and migrated positions of a horizontal reflector.

Figure 4. Influence of the parameters ϵ and δ on the SV-wave residual moveout. All three curves are generated with the correct parameters $V_{nmo,T} = 2.420$ km/s and $\sigma = 0.6$. As marked on the plot, the top curve is obtained with an erroneous δ_M ($\delta_M - \delta_T = 0.1$), the middle curve with erroneous ϵ_M and $\delta_M (\epsilon_M - \epsilon_T = \delta_M - \delta_T = 0.1)$, and the bottom curve with an erroneous $\epsilon_M (\epsilon_M - \epsilon_T = 0.1)$. The correct values are $\epsilon_T = 0.1$ and $\delta_T = -0.1$.

controlled by the NMO velocity and is practically independent, not just of ϵ and δ but also of σ. The sharp increase in the residual moveout for $x/z > 1.7$ in Figure 4 corresponds to the vicinity of the SV-wave velocity maximum where the traveltime $(t^2 - x^2)$ curve rapidly changes its slope (Figures 1 and 2).

At even larger offsets, the residuals for the model with an erroneous δ (top curve, Figure 4) return almost to zero. Even for more pronounced distortions in δ than those in Figure 4, the magnitude of the SV-wave residual moveout stays relatively small for the whole offset range. The contribution of ϵ to long-spread moveout, however, is not negligible and must be examined further.

Next, we study common-image gathers (CIGs) after prestack depth migration for the model in Figure 5. As expected, migration with the actual model parameters (V_{nmo}, σ, ϵ, and δ) produces a near-perfect image for both horizontal and dipping reflectors (Figure 6). The influence of errors in the two main SV-wave kinematic parameters, V_{nmo} and σ, is illustrated in Figure 7. In agreement with the earlier discussion, the correct
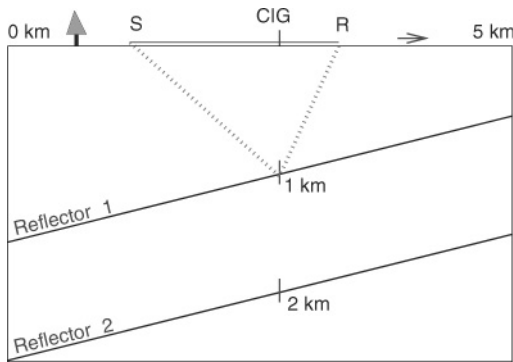

Figure 5. Geometry of the model used in the numerical tests. Two parallel plane reflectors are embedded in a VTI medium, with the dip varying for different models between $0°$ and $40°$. The CIGs in all subsequent tests are displayed at the location where the depths of the two reflectors are 1 and 2 km; the maximum offset is 3 km.
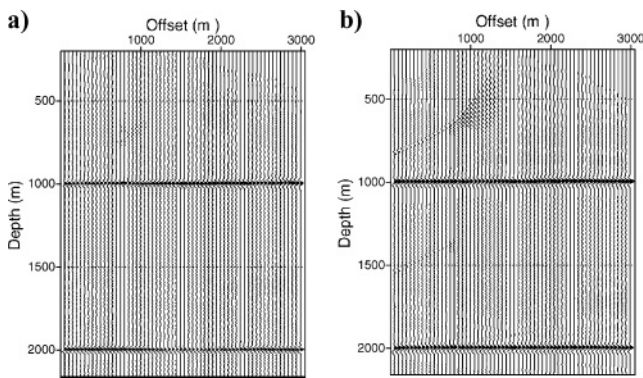
velocity V_{nmo} flattens the events up to a sizable offset-to-depth ratio of about 1.7, whether or not the value of σ is accurate (Figure 7a). For the shallow reflector, the residual moveout in Figure 7a rapidly increases at larger offsets because of the erroneous value of σ. The deeper event, however, remains flat for the whole offset range since the offset-to-depth ratio for it does not exceed 1.5. Figure 7b, in contrast, shows that the residual moveout caused by errors in V_{nmo} influences the entire offset range. Notice that neither event in Figure 7 is imaged at the correct depth (1 km and 2 km) because r in equation 3 is not equal to unity.

These results are similar to those obtained by Sarkar and Tsvankin (2003) for P-wave image gathers migrated using erroneous V_{nmo} or η, yet they differ in two important ways. First, for migration with erroneous σ but the correct NMO velocity (Figure 7a), horizontal SV events stay flat out to a large offset, $x/z \approx 1.7$. The second difference is the abrupt change and rapid increase in the residual moveout of the SV events beyond this offset. Compare Figure 7a with Figure 2a in Sarkar and Tsvankin (2003), where the residual moveout caused by an error in η increases gradually, starting at an offset-to-depth ratio of about one.

The test in Figure 4 indicates that the parameter ϵ (and possibly δ) may contribute to the migrated depth at large offsets. The influence of ϵ and δ on the residual moveout of horizontal SV events is illustrated further by Figures 8 and 9. Although the residual moveout at $x/z > 1.7$ increases almost linearly with errors in both ϵ and δ, the sensitivity of SV-wave image gathers to δ is much weaker (Figure 8). Erroneous values of ϵ, however, lead to nonnegligible residual moveout (Figure 9), which may complicate the estimation of σ from long-spread SV data; this issue is discussed in more detail later on.

Figures 8 and 9 also illustrate one of the key differences between P- and SV-wave image gathers in VTI media: when both the correct V_{nmo} and σ (but perhaps erroneous ϵ and δ) are used in the migration, the horizontal SV events are placed at the true depth. For P-waves, using the correct values of V_{nmo} and η does not ensure that the vertical velocity and, therefore, reflector depth are correct.

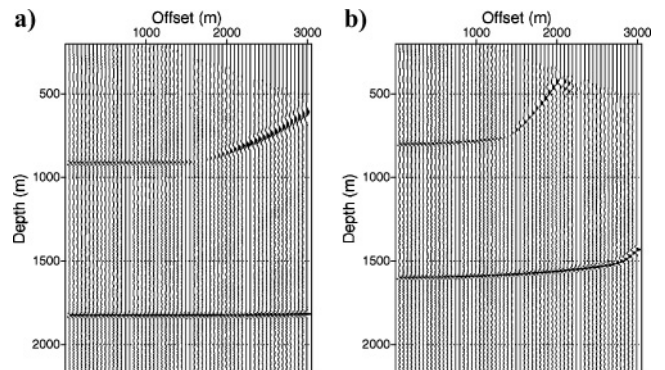Hence, the long-spread moveout of horizontal SV events in image gathers depends not just on V_{nmo} and σ but also on ϵ.

Figure 6. CIGs of SV events in a homogeneous VTI medium after prestack depth migration. The reflectors are (a) horizontal and (b) dipping at $40°$. Migration was performed with the correct model parameters: $V_{P0,T} = 2.420$ km/s, $V_{S0,T} = 1.875$ km/s, $\epsilon_T = 0.1$, and $\delta_T = -0.1$ ($V_{nmo,T} = 2.420$ km/s, $\sigma_T = 0.333$).

Figure 7. Influence of errors in V_{nmo} and σ on CIGs of horizontal SV events. In (a), V_{nmo} is correct but σ is erroneous ($\sigma_M = 0.5$); in (b), σ is correct but V_{nmo} is erroneous ($V_{nmo,M} = 1.936$ m/s). The correct parameters are $V_{nmo,T} = 2.420$ km/s and $\sigma_T = 0.333$.

Although the influence of ϵ implies that this parameter potentially may be constrained by SV-wave traveltimes, it is much more important to estimate the parameter σ. Since V_{nmo} can be obtained with high accuracy from conventional-spread SV data, reliable evaluation of σ would make it possible to determine the vertical velocity V_{S0} and reflector depth (see equation 2). Therefore, we next examine more closely the variation of SV-wave residual moveout with both σ and ϵ.
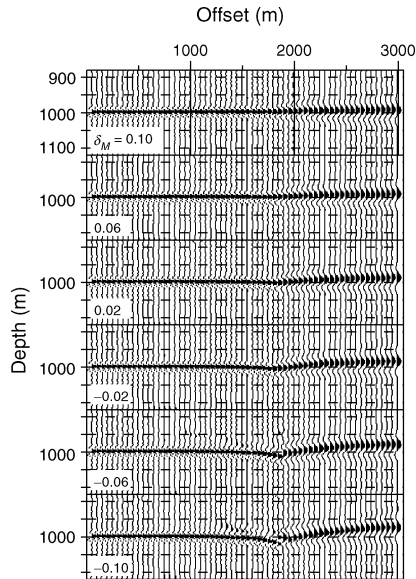

Figure 8. Influence of errors in δ on the residual moveout of a horizontal SV event. The gathers were generated for a range of δ_M values ($\delta_T = 0.1$) and the correct parameters $V_{\text{nmo,T}} = 2.420$ km/s, $\sigma_T = 0.6$, and $\epsilon_T = 0.16$.
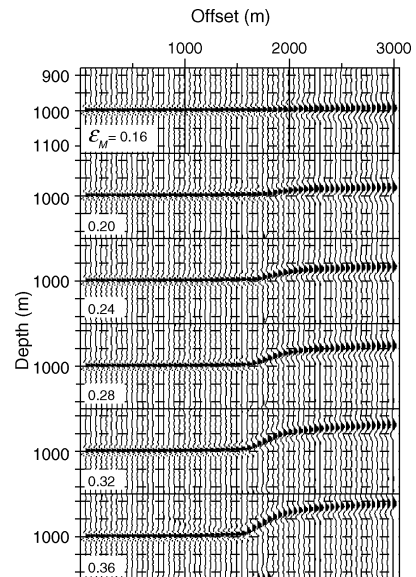

Figure 9. Influence of errors in ϵ on the residual moveout of a horizontal SV event. The gathers were generated for a range of ϵ_M values ($\epsilon_T = 0.16$) and the correct parameters $V_{\text{nmo,T}} = 2.420$ km/s, $\sigma_T = 0.6$, and $\delta_T = 0.1$.

Suppose our goal is to estimate σ by flattening long-spread SV-wave moveout in image gathers. Unless we have a priori information, the value of ϵ used in the migration would be erroneous (as in Figure 10, where $\epsilon_M - \epsilon_T = 0.2$). Note the substantial residual moveout on the panel with the correct $\sigma = 0.6$; consequently, the processor would likely try changing σ to flatten the event. In Figure 10, the smallest residual moveout is observed for distorted values of σ between 0.5 and 0.55, which exemplifies a certain degree of interplay between σ and ϵ. Although none of the gathers for $0.5 < \sigma < 0.55$ is perfectly flat, the residual moveout for this range of σ values may not be detectable on field data in the presence of noise, lateral heterogeneity, and near-surface anomalies, especially if the offset range is more limited than that in Figure 10. Therefore, the tradeoff between σ and ϵ may distort estimates of σ by about 0.1, which would cause unacceptable errors (exceeding 5%) in the vertical velocity and time-to-depth conversion.

Dipping events

Next, consider SV-wave image gathers for a dipping reflector overlaid by a homogeneous VTI layer. Figure 11 shows
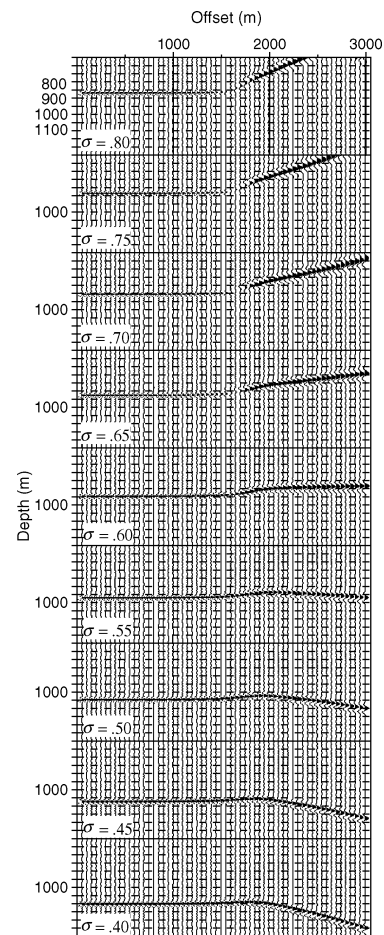

Figure 10. Trade-off between the parameters σ and ϵ for long-spread horizontal events. The image gathers are computed for a range of σ values ($\sigma_T = 0.6$) with erroneous $\epsilon_M = 0.36$ ($\epsilon_T = 0.16$). The NMO velocity was fixed at the correct value, $V_{\text{nmo,T}} = 2.420$ km/s.

that the magnitude of nonhyperbolic moveout of SV-waves in the dip plane of the reflector rapidly increases for dips approaching 40°, where the error of the hyperbolic moveout equation has the opposite sign compared to that for mild dips. The magnitude of nonhyperbolic moveout for dip $\phi = 40°$ is so large that the hyperbolic equation breaks down at offsets of less than one-half the reflector depth. The moveout curve approaches the hyperbola again for dips exceeding 60°.

The anomalous behavior of SV-wave moveout at intermediate dips is caused by small values of the NMO velocity $V_{nmo}(\phi)$, which are predicted by the weak-anisotropy approximation for $V_{nmo}(\phi)$ in Tsvankin (2001, his equation 3.24). The pronounced reduction in the NMO velocity for dips close to 40° (Figure 12), accompanied by a rapid increase in the quartic moveout term, causes the traveltime series $t^2(x^2)$ to break down. For horizontal reflectors, $V_{nmo}(\phi = 0)$ goes to zero when $\sigma = -0.5$ (equation 2), and the SV-wave moveout curve has a shape similar to that for $\phi = 40°$ in Figure 11 [compare Figure 11 here with Figure 4.11 in Tsvankin (2001)]. The increase in the magnitude of nonhyperbolic moveout for a wide range of dips indicates that flattening dipping SV events may require more than one parameter (i.e., more than the dip-dependent NMO velocity) even for moderate offset-to-depth ratios.

This dip dependence of the SV-wave moveout is completely different from that for P-waves. As shown by Tsvankin (2001) and Pech et al. (2003), the magnitude of the P-wave nonhyperbolic moveout initially decreases with dip and goes to zero for a dip close to 30°. The weak-anisotropy approximation for the quartic moveout coefficient A_4 derived by Pech et al. (2003, their equation 19), which can be adapted for SV-waves by replacing η with $(-\sigma)$, predicts the same variation with dip for the moveout of SV-waves. These analytic results, however, do not apply to SV-waves for dips between 25° and 50° because the Taylor series for traveltime becomes inaccurate, and nonhyperbolic moveout is no longer described by the approximate coefficient A_4.

Since the NMO velocity of dipping events depends not only on the zero-dip value (V_{nmo}) but also on the anisotropic parameters, errors in σ lead to residual moveout even at small offsets (Figure 13). As was the case for horizontal events, the velocity V_{nmo} influences the moveout from dipping reflectors for the entire offset range (Figure 14).

It is noteworthy that the residual moveout of dipping events gradually increases with offset (Figures 13b–d and 14b–d), while for horizontal events this increase is abrupt (Figures 13a and 14a). Figures 13 and 14 also show that the moveout residuals at far offsets initially decrease with dip and reach a minimum at about 25°; in contrast, the increase of the residual moveout with dip in the small-to-medium offset range is monotonic. Overall, the dependence of the SV-wave residual
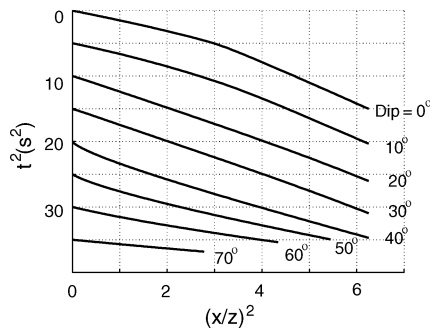
Figure 11. Exact long-spread SV-wave moveout from dipping reflectors for the model of Dog Creek Shale (Thomsen, 1986). The parameters are $V_{P0} = 1.875$ km/s, $V_{S0} = 0.826$ km/s, $\epsilon = 0.225$, and $\delta = 0.1$ ($\sigma = 0.644$). The curves are computed in the dip plane of the reflector for the dips marked on the plot and shifted vertically to avoid crossings. The offset x is normalized by the distance z from the CMP to the reflector.
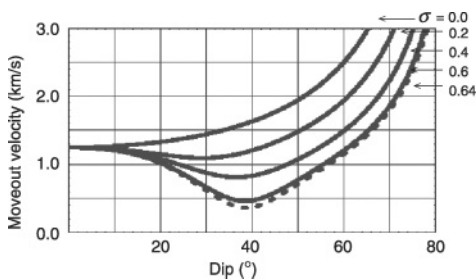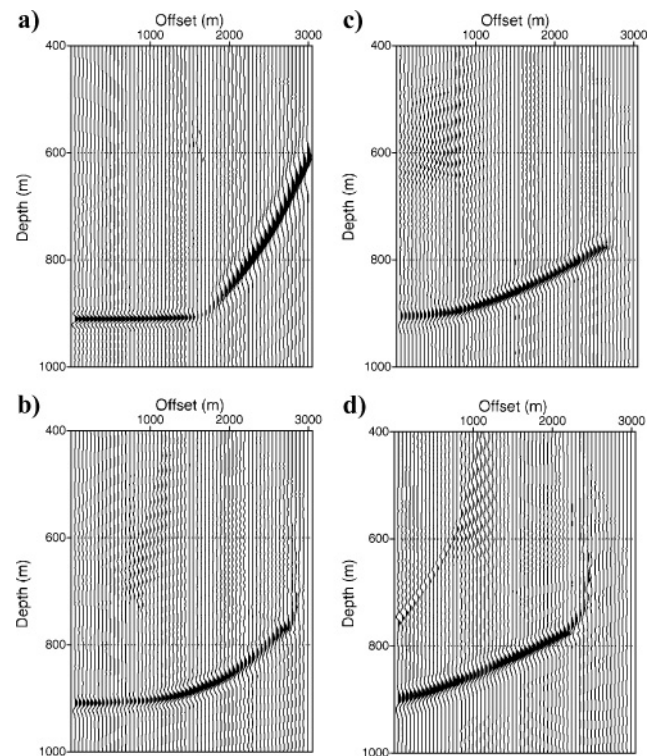
Figure 12. Exact dip-dependent NMO velocity of SV-waves as a function of dip for models with the values of σ marked on the plot. The dashed curve corresponds to the model of Dog Creek Shale with $\sigma = 0.644$ used in Figure 11. The other parameters are $V_{nmo} = 1.875$ km/s, $\epsilon = 0.225$, and $\delta = 0.1$.

Figure 13. Influence of errors in σ on the residual moveout of a dipping event. The test in Figure 7a is repeated here for the shallow reflector, this time dipping at (a) 0°, (b) 20°, (c) 30°, and (d) 40°. The parameter $\sigma_M = 0.5$, while the actual value $\sigma_T = 0.333$; the rest of the model parameters are correct ($V_{nmo,T} = 2.420$ km/s, $\epsilon_T = 0.1$, and $\delta_T = -0.1$).

moveout on errors in V_{nmo} and σ differs substantially from that of the P-wave moveout on errors in the P-wave NMO velocity and η (Sarkar and Tsvankin, 2003).

With both V_{nmo} and σ contributing to the residual moveout of dipping events over a wide range of offsets, we can expect a degree of trade-off between these two parameters. Figure 15 confirms that errors in V_{nmo} can indeed be compensated by errors in σ and that a dipping event can be flattened out to an offset-to-depth ratio of $x/z = 2.5$ using a vastly erroneous migration model.

Whereas δ has even less influence on dipping SV events than on horizontal ones, the contribution of ϵ to the residual moveout represents an additional source of nonuniqueness in parameter estimation. For dipping events, errors in ϵ can produce depth distortions even at small offsets, with the shape and magnitude of the residual moveout strongly dependent on dip. On the whole, the character of the trade-off between σ and ϵ changes with dip, but the general conclusion regarding errors in σ related to a realistic uncertainty in ϵ remains valid for a wide range of dips. Therefore, the SV-wave moveout from a single dipping reflector is insufficient for estimating any of the model parameters without a priori information.

It may be possible, however, to resolve the trade-off between σ and ϵ if SV reflections from both horizontal and dipping interfaces are available (e.g., in the presence of fault planes; see Alkhalifah and Tsvankin, 1995). The image gathers of dipping events in Figure 16 are computed for erroneous values of ϵ and σ that produce an almost flat gather of a horizontal SV event (Figure 10). While the residual moveout is still relatively small for dips of 10° and 20°, it becomes much more significant when the dip exceeds 30°. Note that combining the P-wave NMO velocities of horizontal and dipping events provides a stable way of estimating the parameter η in vertically heterogeneous VTI media (Alkhalifah and Tsvankin, 1995; Tsvankin, 2001). The main difference between the P-wave DMO inversion algorithm and the moveout analysis of

Figure 15. Image gathers of a dipping event ($\phi = 20°$) obtained using erroneous values of $V_{\mathrm{nmo,M}} = 2.0$ km/s and σ_M (marked on the plot); the parameters ϵ and δ are correct. The true model parameters are $V_{\mathrm{nmo,T}} = 2.420$ km/s, $\sigma_T = 0.6$, $\epsilon_T = 0.16$, and $\delta_T = 0.1$. The gather for $\sigma_M = 0.15$ is practically flat.
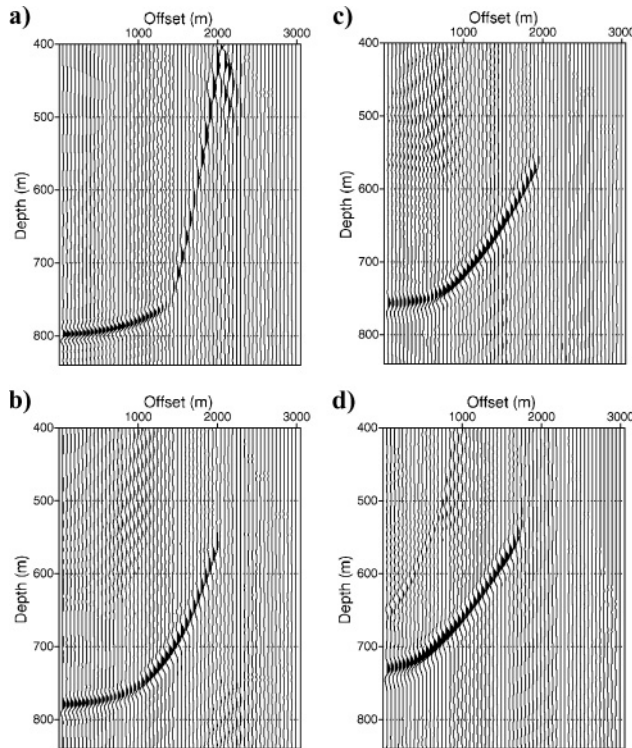

Figure 14. Influence of errors in the zero-dip NMO velocity on the residual moveout of a dipping event. The test in Figure 7b is repeated here for the shallow reflector, this time dipping at (a) 0°, (b) 20°, (c) 30°, and (d) 40°. The velocity $V_{\mathrm{nmo,M}} = 1.936$ km/s, while the actual value $V_{\mathrm{nmo,T}} = 2.420$ km/s; the rest of the model parameters are correct ($\sigma_T = 0.333$, $\epsilon_T = 0.1$, and $\delta_T = -0.1$).
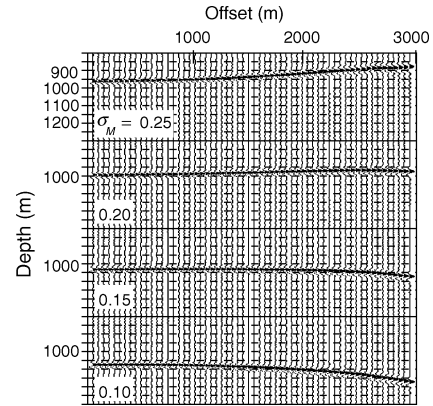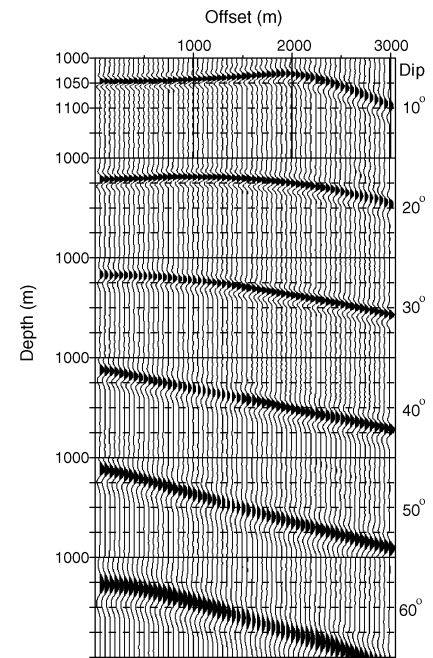

Figure 16. Influence of errors in ϵ and σ on the residual moveout of dipping events (dips are marked on the plot). The migration was performed with $\sigma_M = 0.5$, $\epsilon_M = 0.36$ (see Figure 10), while the correct values are $\sigma_T = 0.6$ and $\epsilon_T = 0.16$. The correct $V_{\mathrm{nmo,T}} = 2.420$ km/s is used throughout.

SV-waves discussed here is the need to use long-spread horizontal SV events that help to constrain σ and ϵ.

Factorized vertically heterogeneous VTI medium

In factorized anisotropic media, the stiffness coefficients vary in space but their ratios are held constant (e.g., Červený, 1989). Factorized models provide an efficient framework for simultaneous study of the influence of heterogeneity and anisotropy on seismic signatures and help to speed up application of such modeling tools as anisotropic ray tracing (Sarkar and Tsvankin, 2003, 2004). Since the Thomsen parameters ϵ, δ, and γ are defined through the ratios of the stiffnesses, they remain spatially invariant in factorized VTI media. The vertical velocities V_{P0} and V_{S0}, however, may change arbitrarily in space as long as V_{P0}/V_{S0} is constant.

We consider a special type of factorized VTI media in which V_{P0} and V_{S0} are linear functions of depth z:

$$V_{P0}(z) = V_{P0}(0) + k_{zp}\, z, \qquad (4)$$

$$V_{S0}(z) = V_{S0}(0) + k_{zs}\, z, \qquad (5)$$

where $V_{P0}(0)$ and $V_{S0}(0)$ are the velocities at the surface ($z = 0$) and k_{zp} and k_{zs} are the vertical-velocity gradients for P- and SV-waves, respectively. According to equations 4 and 5, for the ratio $V_{P0}(z)/V_{S0}(z)$ to be independent of z, the gradients have to satisfy the condition $k_{zp}/k_{zs} = V_{P0}(0)/V_{S0}(0)$. Hence, the velocity gradient for P-waves in factorized $v(z)$ VTI media should be much higher than that for SV-waves.

The NMO velocity of SV-waves from a horizontal reflector can be found as a function of the vertical reflection time t_0 by adapting the corresponding result for P-waves in Sarkar and Tsvankin (2003, their Appendix B). Their equation 6 for the P-wave NMO velocity remains valid for SV-waves if we replace the velocity gradient k_{zp} by k_{zs}:

$$V_{\mathrm{nmo}}^2(t_0) = \frac{V_{\mathrm{nmo}}^2(t_0 = 0)}{t_0\, k_{zs}}\left(e^{t_0\, k_{zs}} - 1\right), \qquad (6)$$

where $V_{\mathrm{nmo}}(t_0 = 0) = V_{S0}(0)\sqrt{1 + 2\sigma}$ is the SV-wave NMO velocity at the surface.

For moveout analysis of SV data, it is convenient to parameterize the factorized medium by the velocity $V_{\mathrm{nmo}}(t_0 = 0)$, gradient k_{zs}, and the anisotropic parameters σ, ϵ, and δ. The P-wave vertical velocity at the surface $V_{P0}(0)$ and gradient k_{zp} would be redundant as model parameters because they can be expressed through the five parameters listed above.

From our equation 6, the correct NMO velocity for a range of vertical times t_0 can be obtained only by setting both the velocity $V_{\mathrm{nmo}}(t_0 = 0)$ and gradient k_{zs} in the migration model to the correct values. The same conclusion is reached for P-wave moveout by Sarkar and Tsvankin (2003); an accurate velocity $V_{\mathrm{nmo}}(t_0)$, however, helps to flatten out horizontal SV events to much larger offsets compared to those for P-waves.

If the migration is performed with the correct values of the five key parameters listed above, both horizontal and dipping events are well imaged and properly positioned (Figure 17). The gathers in Figure 18 were generated for the actual values of $V_{\mathrm{nmo}}(t_0 = 0)$ and the SV-wave gradient k_{zs}, but the vertical velocities at the surface and the P-wave gradient k_{zp} were incorrect. Hence, the migration model is not factorized, and the parameter σ is distorted and varies with depth. As was the case for homogeneous media, errors in σ lead to residual moveout of horizontal events for large offset-to-depth ratios $x/z > 1.7$ as well as to a depth shift (Figure 18a). For dipping events, the influence of σ on the NMO velocity becomes substantial for dips larger than 20°; for a dip of 40°, erroneous σ causes residual moveout for the whole offset range (Figure 18b, c).

The dependence of the residual moveout on the parameters ϵ and δ in vertically heterogeneous media is similar to that discussed for homogeneous models. The contribution of δ to SV-wave moveout is practically negligible, while ϵ must be taken into account when migrating dipping events and long-offset reflections from horizontal interfaces.

Therefore, the model parameters needed in the depth migration of SV-waves in factorized $v(z)$ media include the NMO velocity at the surface [$V_{\mathrm{nmo}}(t_0 = 0)$], the gradient k_{zs}, and the anisotropic parameters σ and ϵ. The velocity $V_{\mathrm{nmo}}(t_0 = 0)$ and gradient k_{zs} can be found from conventional-spread moveout for two reflectors sufficiently separated in depth, as

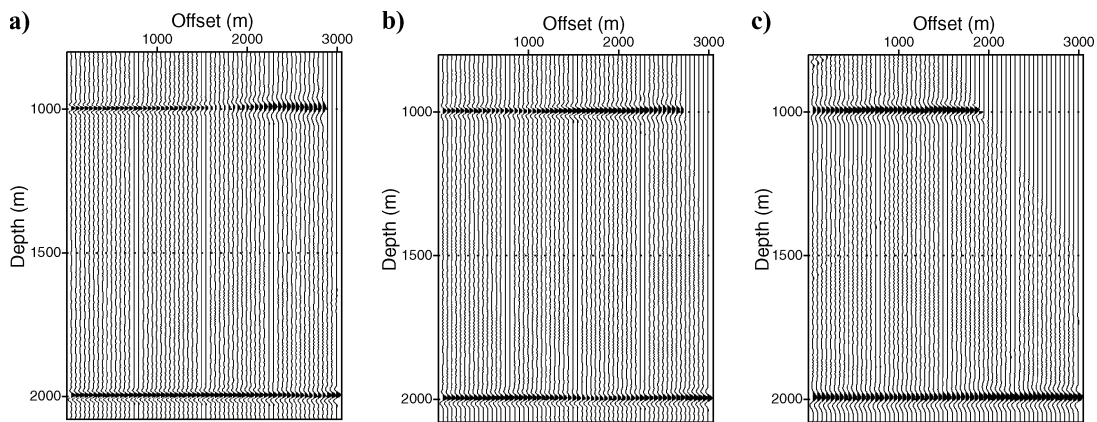Figure 17. SV-wave image gathers for two reflectors embedded in a factorized $v(z)$ VTI medium. The reflector dips are (a) 0°, (b) 20°, and (c) 40°. The migration was performed with the actual model parameters: $V_{P0,T}(z = 0) = 2.420$ km/s, $k_{zp,T} = 0.4\,\mathrm{s}^{-1}$, $V_{S0,T}(z = 0) = 1.875$ km/s, $k_{zs,T} = 0.31\,\mathrm{s}^{-1}$, $\epsilon_T = 0.1$, and $\delta_T = -0.1$ [$V_{\mathrm{nmo,T}}(t_0 = 0) = 2.420$ km/s, $\sigma_T = 0.333$]. The far offsets are muted to remove migration artifacts caused by the limited lateral extent of the model.
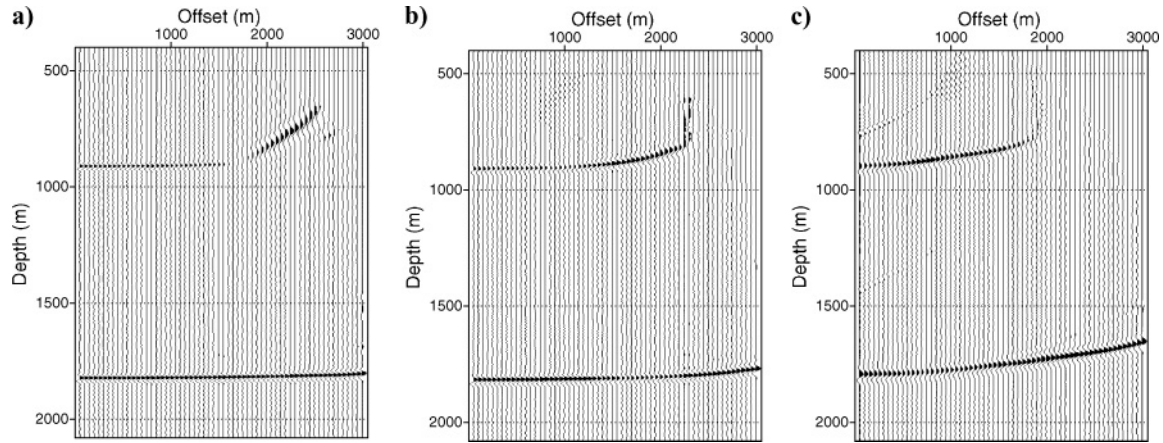
Figure 18. Influence of errors in σ on image gathers in $v(z)$ VTI media. The true (factorized) model is the same as that in Figure 17; the dips are (a) $0°$, (b) $20°$, and (c) $40°$. The migration was performed with the parameters $V_{P0,M}(z=0) = 2.707$ km/s, $V_{S0,M}(z=0) = 1.712$ km/s, $k_{zp,M} = 0$, $k_{zs,M} = 0.31$ s^{-1}, $\epsilon_M = 0.2$, and $\delta_M = 0$. The SV-wave function $V_{\mathrm{nmo}}(t_0)$ in the migration model is correct $[V_{\mathrm{nmo,M}}(t_0=0) = V_{\mathrm{nmo,T}}(t_0=0) = 2.420$ km/s; $k_{zs,M} = k_{zs,T} = 0.31$ s$^{-1}]$, but σ_M varies from 0.5 at the surface to 0.437 at a depth of 3 km ($\sigma_T = 0.333$).

suggested by Sarkar and Tsvankin (2003, 2004) for P-wave data. Although the SV-wave residual moveout is not highly sensitive to ϵ, we still observe a trade-off between σ and ϵ that may distort estimates of σ and the vertical velocity V_{S0} using long-spread horizontal events.

DISCUSSION AND CONCLUSIONS

SV-wave data are strongly influenced by elastic anisotropy and can provide valuable information for migration velocity analysis in VTI media. The goal of this paper is to study the residual moveout of SV events after prestack depth migration and identify the parameters responsible for the quality of the migration result over a wide range of reflector dips. An analytic solution for SV-wave moveout in image gathers can be adapted from the weak-anisotropy approximation for P-waves. This linearized formula, however, is not sufficiently accurate for shear waves, so we carried out numerical analysis of SV-wave image gathers by performing prestack depth migration for a representative set of VTI models.

For homogeneous VTI media, the moveout of both horizontal and dipping SV events in image gathers is mostly controlled by two main parameters: the zero-dip NMO velocity V_{nmo} and the anisotropic parameter σ. The hyperbolic portion of the moveout curve for horizontal SV events, which extends out to relatively large offset-to-depth ratios of about 1.7, is dependent on just V_{nmo}. Therefore, small- and moderate-spread SV-wave gathers can be flattened using the correct NMO velocity without knowledge of the anisotropic parameters or the vertical S-wave velocity V_{S0}.

Erroneous values of σ lead to an abrupt increase in the residual moveout for offsets approaching twice the reflector depth, which potentially could be used to estimate both V_{nmo} and σ using SV reflections from horizontal interfaces. Since the combination of V_{nmo} and σ yields the velocity V_{S0}, it may seem that flattening long-spread SV gathers can help to con-

strain reflector depth. Accurate estimation of σ, however, is hampered by the influence of the parameter ϵ on long-spread residual moveout (the contribution of δ is inconsequential). The interplay between σ and ϵ in the removal of residual moveout at large offsets can cause errors in σ of about 0.1, which is unacceptable for time-to-depth conversion.

The correct parameters V_{nmo}, σ, and ϵ are also needed to flatten SV events from dipping reflectors in homogeneous VTI media. In the presence of dip, however, σ makes a substantial contribution to the near-offset moveout as well. The magnitude of the far-offset residual moveout for a fixed error in V_{nmo} or σ reaches its minimum for reflectors with intermediate dips ($20°–40°$ in our examples).

For factorized $v(z)$ VTI models with constant vertical-velocity gradient, it is convenient to perform moveout analysis using the following five parameters: the SV-wave NMO velocity at the surface $V_{\mathrm{nmo}}(t_0=0)$, the gradient k_{zs} in the S-wave vertical velocity, and the anisotropic parameters σ, ϵ, and δ. Flattening conventional-spread horizontal SV events for a range of vertical times requires migration with the correct values of $V_{\mathrm{nmo}}(t_0=0)$ and k_{zs}. As is the case for homogeneous media, the moveout on long-spread gathers also depends on σ and ϵ, with a certain degree of trade-off between these two parameters. Note that the factorized model may not be realistic for shear-wave analysis because it involves a fixed (and possibly artificial) relationship between the velocity gradients of P- and SV-waves.

Table 1 summarizes the results of our analysis of the SV-wave residual moveout. The parameters needed to flatten horizontal and dipping SV events in image gathers are listed along with their P-wave counterparts for both homogeneous and factorized $v(z)$ VTI media.

The main obstacle in the depth-domain velocity analysis of SV data is apparently the trade-off between the parameters σ and ϵ on long-spread gathers. While the SV-wave NMO velocity is tightly constrained by moderate-spread moveout of horizontal events, the influence of ϵ on long-spread data may

Table 1. Model parameters needed to flatten P and SV events in long-spread image gathers.

Medium type	P-wave	SV-wave
Homogeneous VTI	$V_{\mathrm{nmo,P}}$	$V_{\mathrm{nmo,SV}}$
	η	σ
		ϵ
Factorized $v(z)$ VTI	$V_{\mathrm{nmo,P}}(0)$	$V_{\mathrm{nmo,SV}}(0)$
	k_{zp}	k_{zs}
	η	σ
		ϵ

prevent us from estimating σ and, therefore, the vertical velocity with sufficient accuracy. One possible way to resolve this ambiguity, which should be explored in migration velocity analysis algorithms, is to combine horizontal and dipping events (the dips should exceed $25°$). The accuracy of the inversion of SV data can also be increased if an estimate of the ratio of the vertical P- and S-wave velocities is available.

Still, the problems in estimating the parameter σ and the depth scale of the model using solely SV-wave data highlight the need for a joint velocity analysis of P- and SV-waves. All relevant VTI parameters (V_{P0}, V_{S0}, ϵ, and δ) and reflector depth can be constrained by combining long-spread P and SV reflection traveltimes from horizontal interfaces. Implementation of this approach in the migrated domain will require a search for a model that flattens P- and SV-wave image gathers simultaneously and ensures that the P and SV migrated sections are tied in depth.

REFERENCES

Alkhalifah, T., 1995a, Efficient synthetic-seismogram generation in transversely isotropic, inhomogeneous media: Geophysics, **60**, 1139–1150.

———, 1995b, Gaussian beam depth migration for anisotropic media: Geophysics, **60**, 1474–1484.

Alkhalifah, T., and I. Tsvankin, 1995, Velocity analysis for transversely isotropic media: Geophysics, **60**, 1550–1566.

Al-Yahya, K., 1987, Prestack migration velocity analysis: Determination of interval velocities: Stanford Exploration Project SEP-51, 49–61.

Červený, V., 1989, Ray tracing in factorized anisotropic inhomogeneous media: Geophysical Journal International, **99**, 91–100.

Grechka, V., and P. Dewangan, 2003, Generation and processing of pseudo shear-wave data: Theory and case study: Geophysics, **68**, 1807–1816.

Grechka, V., and I. Tsvankin, 2002a, PP + PS = SS: Geophysics, **67**, 1961–1971.

———, 2002b, The joint nonhyperbolic moveout inversion of PP and PS data in VTI media: Geophysics, **67**, 1929–1932.

Grechka, V., A. Pech, and I. Tsvankin, 2002, Multicomponent stacking-velocity tomography for transversely isotropic media: Geophysics, **67**, 1564–1574.

Liu, Z., 1997, An analytical approach to migration velocity analysis: Geophysics, **62**, 1238–1249.

Pech, A., I. Tsvankin, and V. Grechka, 2003, Quartic moveout coefficient: 3D description and application to tilted TI media: Geophysics, **68**, 1600–1610.

Sarkar, D., and I. Tsvankin, 2003, Analysis of image gathers in factorized VTI media: Geophysics, **68**, 2016–2025.

———, 2004, Migration velocity analysis in factorized VTI media: Geophysics, **69**, 708–718.

Thomsen, L., 1986, Weak elastic anisotropy: Geophysics, **51**, 1954–1966.

———, 1999, Converted-wave reflection seismology over inhomogeneous, anisotropic media: Geophysics, **64**, 678–690.

Tsvankin, I., 2001, Seismic signatures and analysis of reflection data in anisotropic media: Elsevier Science Publishing Co., Inc.

Tsvankin, I., and L. Thomsen, 1994, Nonhyperbolic reflection moveout in anisotropic media: Geophysics, **59**, 1290–1304.

———, 1995, Inversion of reflection traveltimes for transverse isotropy: Geophysics, **60**, 1095–1107.